

Received Date : 30-Apr-2016

Revised Date : 28-Jun-2016

Accepted Date : 02-Jul-2016

Article type : Research Article

## Design, synthesis and preliminary bioactivity evaluations of *N*<sup>1</sup>-hydroxyterephthalamide derivatives with indole cap as novel histone deacetylase inhibitors

Xue Wang<sup>a</sup>, Xiaoyang Li<sup>a</sup>, Jingyao Li<sup>a</sup>, Jinning Hou<sup>a</sup>, Ying Qu<sup>a</sup>, Chenggong Yu<sup>a</sup>, Feng He<sup>a</sup>, Wenfang Xu<sup>a</sup>, Jingde Wu<sup>a\*</sup>

<sup>a</sup> Department of Medicinal Chemistry, School of Pharmaceutical Sciences, Shandong University, 44 West Culture Road, 250012 Ji'nan, Shandong, PR China

Corresponding author, Tel: +86-531-88382006; Fax:+86-531-88382006, E-mail: wujingde70@sdu.edu.cn, jingdewu70@gmail.com.

### Abstract

Histone deacetylases inhibitors (HDACIs) have been widely recognized as significant therapeutic approach to cancers. In our efforts to develop novel histone deacetylases inhibitors (HDACIs) as potential anticancer agents, a series of *N*<sup>1</sup>-hydroxyterephthalamide derivatives with an indole cap group were designed and synthesized. Compound **12m** was identified to be the most potent one (IC<sub>50</sub>=0.074μM against Hela nuclear extracts) and showed higher inhibitory activity than the positive control **SAHA** (IC<sub>50</sub>=0.131μM), which

This article has been accepted for publication and undergone full peer review but has not been through the copyediting, typesetting, pagination and proofreading process, which may lead to differences between this version and the Version of Record. Please cite this article as doi: 10.1111/cbdd.12819

This article is protected by copyright. All rights reserved.

was also verified by further molecular docking studies into active site of HDAC2. The results of selectivity on the inhibition of HDACs exhibited **12m** being with comparable similar overall isoform selective profile with PXD101. In addition, the representative compounds based on the outcomes of preliminary tumor cell screening demonstrated more potent or comparable to **SAHA** in the next antiproliferative activity assays. Collectively, the results encouraged further development of this chemical template to provide more potent analogs as HDACIs.

**Keywords:** HDACIs, molecular docking, antiproliferative activity, selectivity

## 1. Introduction

The epigenetic abnormality is determined by chromatin structure including DNA methylation, histone variants and modifications, nucleosome remodeling as well as small non-coding regulatory RNAs, and viewed as another pathway to initiation and progression of cancer based on genetic mutations<sup>1</sup>. Histone deacetylases (HDACs), exert silencing effects on cell-cycle regulatory genes associated with cell proliferation, differentiation and diminishing apoptosis which play a crucial role in the transition of normal cells into malignant cells<sup>2</sup>.

Thus far, 18 HDACs have been identified in humans and categorized into four classes due to their sequence homology to yeast orthologs<sup>3</sup>. Class I, including HDACs 1, 2, 3 and 8, shares homology with Rpd3. Class II can be divided into two subclasses – IIa (HDACs 4, 7 and 9) and IIb (HDACs 6 and 10), which holds homology to HDAC1. Class IV, covers the sole member of HDAC11 and possesses homology with both class I and class II. The 11 family members referred to as classical HDACs, are metal-dependent enzymes inhibited by Zn<sup>2+</sup> ion chelating compounds with differ in the catalytic mechanisms of class III HDACs as these enzymes with homology to the Sir2 (Silent information regulator 2) family requiring NAD<sup>+</sup> as an essential cofactor during catalysis<sup>4</sup>. Although the biological functions of HDAC isoforms have not been fully understood yet, HDACs expression in specific tissues as well as

organs, and their different levels in various types of cancers both contribute to indicate the progress of diseases and develop agents with more precise therapeutic effects<sup>5</sup>.

Up to date, four HDACIs, vorinostat (SAHA)<sup>6</sup>, romidepsin (FK228)<sup>7</sup>, belinostat (PXD101)<sup>8,9</sup> and panobinostat (LBH589)<sup>10</sup> have been approved by the US FDA. SAHA and FK228 are approved for the clinical therapy of cutaneous T-cell lymphoma (CTCL), PXD101 is for the treatment of peripheral T-cell lymphoma (PTCL) and LBH589 is applied for combination therapy with bortezomib and dexamethasone for the treatment of recurrent multiple myeloma<sup>11</sup>. Additionally, over 20 HDACIs were in diverse clinical trials during the past 10 years. In general, numerous HDACIs share a common pharmacophore model which consists of three portions: zinc ion binding group (ZBG) that chelates zinc ion of HDACs active site; hydrophobic opposite capping group that enhances the affinity with residues of external HDACs and a linker, connecting ZBG and cap group (**Fig. 1**)<sup>12</sup>.

Olson and co-workers reported that compound **2**<sup>b13</sup> exhibited potent HDACs inhibitory activity and excellent selectivity for HDAC2 (IC<sub>50</sub>=0.61 μM) and HDAC6 (IC<sub>50</sub>=0.004 μM), thus suggesting that the *N*<sup>1</sup>-hydroxyterephthalamide could be an ideal moiety in the design of effective HDACIs. Indole structure appears frequently in molecule drug design<sup>14, 15</sup> and has been successfully employed in design of potent HDACIs such as the FDA-approved panobinostat and Quisinostat that is under clinical trial (JNJ-26481585)<sup>16,17</sup>. Our laboratory is also interested in exploring the indole-containing cap group in designing novel HDACIs. For example, compound **14a**<sup>18</sup> exhibited potent in vitro and in vivo anti-cancer activities. In continuation of our efforts to explore this structural feature and design of new HDACIs, herein, we reported the design, synthesis and preliminary bioactivity evaluation of *N*<sup>1</sup>-hydroxyterephthalamide derivatives with indole cap as HDACIs (**Fig. 2**). Preliminary structure-activity relationship (SAR) studies were also discussed.

## 2. Experimental section

### 2.1 Chemistry

All commercially available starting materials, reagents and solvents were used without further purification unless otherwise stated. All reactions were monitored by TLC using 0.25 mm silica gelplates (60GF-254). UV light and ferric chloride were used to visualize the spots.  $^1\text{H}$  NMR spectra were obtained on a Bruker DRX spectrometer at 400 MHz or 300 MHz with TMS as an internal standard,  $\delta$  in parts per million and J in hertz. High-resolution mass spectrometry was performed by Shandong Analysis and Test Center in Ji'nan, China. ESI-MS spectra were recorded on an API 4000 spectrometer. Silica gel was used for column chromatography purification. Flash chromatography was accomplished using the automated Combi Flash Rf system from Teledyne ISCO and was done using silicagel of 200-300 mesh. Melting points were determined on an electro thermal melting point apparatus.

#### 2.1.1 General Procedure for the Preparation of **2**

##### *(Tert-Butoxycarbonyl)-L-tryptophan (2)*

L-Tryptophan (10.2 g, 50 mmol) was dissolved in 1 M NaOH (100 mL) aqueous solution, then solution of  $\text{Boc}_2\text{O}$  (13.08 g, 60 mmol) in THF was added dropwise. After the reaction finished, THF was evaporated. The residual aqueous solution was acidified with 1 N HCl until pH 3-4 and then extracted with EtOAc (3×100 mL). The organic layer was washed with brine (2×50 mL) and dried over  $\text{Na}_2\text{SO}_4$  overnight, then evaporated under vacuum to obtained white solid **2**, which was directly used in the next step without further purification.

### 2.1.2 General Procedure for the Preparation of 3

#### *(S)-benzyl 2-((tert-butoxycarbonyl)amino)-3-(1H-indol-3-yl)propanoate (3)*

To a solution of **2** (9 g, 30 mmol) in anhydrous CH<sub>2</sub>Cl<sub>2</sub> (150 ml), was added HOBT (4.8 g, 36 mmol) and EDCI (6.9 g, 36 mmol) at 0°C, followed by Et<sub>3</sub>N (3.6 g, 36 mmol). After 30 min, phenylmethanol (3.9 g, 36 mmol) was added 30 min later. After 9 h, the solution of CH<sub>2</sub>Cl<sub>2</sub> was washed with 1 M HCl (2×40 mL), saturated Na<sub>2</sub>CO<sub>3</sub> (2×40 mL) and brine (2×40 mL), dried over MgSO<sub>4</sub> overnight, and the solvent was evaporated under vacuum to afford white solid **3**, which was directly used in the next step without further purification.

### 2.1.3 General Procedure for the Preparation of 4

#### *(S)-Benzyl 2-amino-3-(1H-indol-3-yl) propanoatehydrochloride (4)*

Compound **3** (9.9 g, 25 mmol) was dissolved in a solution of EtOAc (100 mL) saturated by dry HCl gas. The solution was stirred at room temperature overnight. The filtered precipitate was washed by diethyl ether to give the white solid powder **4**, which was directly used in the next step without further purification.

### 2.1.4 General Procedure for the Preparation of 5

#### *(S)-Methyl-4-((1-(benzyloxy)-3-(1H-indol-3-yl)-1-oxopropan-2-yl) carbamoyl) ben-zoate (5)*

To a solution of 4-(methoxycarbonyl)benzoic acid (3.6 g, 20 mmol) in anhydrous CH<sub>2</sub>Cl<sub>2</sub>, was added 2-(1H-Benzotriazole-1-yl)-1,1,3,3-tetramethyluronium tetrafluoroborate (TBTU, 7.7 g, 24 mmol), followed by Et<sub>3</sub>N (2.4 g, 24 mmol). After 30 min, compound **4** (6.6 g, 20 mmol) was added followed by Et<sub>3</sub>N (2.4 g, 24 mmol). 4 h later, the solution of CH<sub>2</sub>Cl<sub>2</sub> was washed with 1 M HCl (2×40 mL), saturated Na<sub>2</sub>CO<sub>3</sub> (2×40 mL) and brine (2×40 mL), dried

over MgSO<sub>4</sub> overnight and evaporated under vacuum. The desired compound **5** was derived by crystallization in EtOAc as white powder.

### 2.1.5 General Procedure for the Preparation of **6**

#### *(S)*-3-(1*H*-indol-3-yl)-2-(4-(methoxycarbonyl) benzamido) propanoic acid (**6**)

Compound **5** (6.8 g, 15 mmol) was dissolved in 200 mL MeOH, and then Pd/C of 0.68 g was added. The solution was stirred at room temperature overnight under the atmosphere of hydrogen, then was filtered with diatomite, evaporated under vacuum and washed by diethyl ether to give white solid **6**, which was directly used in the next step without further purification.

### 2.1.6 General Procedure for the Preparation of **7b-h**

#### *(S)*-Methyl-4-((3-(1*H*-indol-3-yl)-1-oxo-1-(propylamino) propan-2-yl) carbamoyl) benzoate (**7b**)

To a solution of compound **6** (0.73 g, 2 mmol) in anhydrous CH<sub>2</sub>Cl<sub>2</sub> (20 ml), was added propan-1-amine (0.12 g, 2 mmol), Benzotriazol-1-yl-oxytripyrrolidino-phosphonium hexafluorophosphate (PyBop, 1.0 g, 2 mmol) at 0°C, followed by Et<sub>3</sub>N (0.2 g, 2 mmol). The solution was stirred at room temperature overnight. The solution was washed with 1 M HCl (2×10 mL), saturated Na<sub>2</sub>CO<sub>3</sub> (2×10 mL) and brine (2×10 mL), dried over MgSO<sub>4</sub> overnight and the solvent was evaporated under vacuum. The desired compound **7b** was derived by crystallization in mixture of EtOAc and petroleum ether as white solid.

Compounds **7c-h** were prepared using the same procedure as described above.

### 2.1.7 General Procedure for the Preparation of 8a-h and 12a-p

*(S)-N<sup>1</sup>-(3-(1H-indol-3-yl)-1-oxo-1-(propylamino) propan-2-yl)-N<sup>4</sup>-hydroxyterephthalamide (8a)*

KOH (38.64 g, 690 mmol) and NH<sub>2</sub>OH HCl (23.35 g, 343 mmol) were dissolved, respectively, in 70 mL and 120 mL MeOH to get solution A and solution B. Next solution A was added drop wise to solution B. After filtering the precipitate (KCl), a NH<sub>2</sub>OK solution was obtained. Compound **6** (0.38 g, 1 mmol) was dissolved in the NH<sub>2</sub>OK solution and stirred overnight. After the reaction was completed, it was evaporated under vacuum. The residue was acidified with 1 N HCl to a pH 3-4 and then extracted with EtOAc (3×20 mL). The organic layer was washed with brine (2×30 mL) and dried over Na<sub>2</sub>SO<sub>4</sub> overnight. The crude material was purified via flash chromatography to afford the light brown solid **8a**.

Compounds **8b-h** and **12a-p** were prepared using the same procedure as described above.

### 2.1.8 General Procedure for the Preparation of 9a-h

*(S)-tert-butyl (3-(1H-indol-3-yl)-1-oxo-1-(phenylamino)propan-2-yl)carbamate (9a)*

Compound **2** (3.0 g, 10 mmol) was dissolved in anhydrous CH<sub>2</sub>Cl<sub>2</sub>, 2-(1H-Benzotriazole-1-yl)-1, 1, 3, 3-tetramethyluronium tetrafluoroborate (TBTU, 3.9 g, 12 mmol) was added, followed by Et<sub>3</sub>N (1.2 g, 12 mmol). After 30 min, aniline (1.1 g, 12 mmol) was added. 4 h later, the solution of CH<sub>2</sub>Cl<sub>2</sub> was washed with 1 M HCl (2 ×20 mL), saturated Na<sub>2</sub>CO<sub>3</sub> (2×20 mL) and brine (2×20 mL), dried over MgSO<sub>4</sub> overnight, and the solvent was evaporated under vacuum, affording white solid **9a**, which was directly used in the next step without further purification.

Compounds **9b-h** were prepared using the same procedure as described above.

### 2.1.9 General Procedure for the Preparation of 10a-h

#### *(S)-2-amino-3-(1H-indol-3-yl)-N-phenyl-propionamide hydrochloride (10a)*

Compound **9a** (3.0 g, 8 mmol) was dissolved in a solution of EtOAc (30 mL) saturated by dry HCl gas. The solution was stirred at room temperature overnight. The filtered precipitate was washed by EtOAc to give white solid powder **10a**, which was directly used in the next step without further purification.

Compounds **10b-h** were prepared using the same procedure as described above.

### 2.1.10 General Procedure for the Preparation of 11a-h

#### *(S)-Methyl-4-((3-(1H-indol-3-yl)-1-oxo-1-(phenylamino) propan-2-yl) carbamoyl) benzoate (11a)*

To a solution of 4-(methoxycarbonyl)benzoic acid (0.9 g, 5 mmol) in anhydrous CH<sub>2</sub>Cl<sub>2</sub>, was added 2-(1H-Benzotriazole-1-yl)-1,1,3,3-tetramethyluronium tetrafluoroborate (TBTU, 1.9 g, 6 mmol), followed by Et<sub>3</sub>N (0.6 g, 6 mmol). After 30 min, compound **10a** (1.6 g, 5 mmol) was added followed by Et<sub>3</sub>N (0.6 g, 6 mmol). The solution was stirred at room temperature overnight, then washed with 1 M HCl (2 × 20 mL), saturated Na<sub>2</sub>CO<sub>3</sub> (2 × 20 mL) and brine (2 × 20 mL), dried over MgSO<sub>4</sub> overnight, and the solvent was evaporated under vacuum to afford white solid **11a**, which was directly used in the next step without further purification.

Compounds **11b-h** were prepared using the same procedure as described above.

### 2.2 *In vitro* HDACs inhibition fluorescence assay

*In vitro* HDACs inhibition assays were conducted as previously described<sup>16</sup>. In brief, 10 μL of Hela nuclear extracts was mixed with various concentrations of target compounds (50 μL), SAHA, using 100% and none HDACs groups as control group, and the mixture. After incubation at 37°C for 10 min, fluorogenic substrate Boc-Lys (acetyl)-AMC (40 μL) was

added and then the mixture was incubated at 37°C for 30 min. The mixture was stopped by addition of 100 µL of developer containing trypsin and TSA afterwards. Over the next incubation at 37°C for 20 min, fluorescence intensity was measured using a microplate reader at excitation and emission wavelengths of 390 nm and 460 nm, respectively. The inhibition ratios were calculated from the fluorescence intensity readings of tested wells relative to those of control wells, and the IC<sub>50</sub> values were calculated using a regression analysis of the concentration/inhibition data.

### 2.3 Molecular Docking Studies

Compounds were docked into the active site of HDAC2 (PDB entry: 4LXZ) using Tripos sybyl x 2.0. Before the docking process, the protein structure was treated by deleting water molecules, adding hydrogen atoms, fixing atom types, and assigning AMBER7 FF99 charges. A 100-step minimization process was performed to further optimize the protein structure. The molecular structures were generated with the Sybyl/Sketch module and optimized using Powell's method with the Tripos force field with convergence criterion set at 0.05 kcal/(Å mol) and assigned charges with the Gasteiger\_Hückel method. Molecular docking was carried out *via* the Sybyl/FlexX module. Other docking parameters were kept to the default values.

### 2.4 *In vitro* antiproliferative assay

*In vitro* antiproliferative assays were determined by the MTT (3-[4,5-dimethyl-2-thiazolyl]-2,5-diphenyl-2H-tetrazolium bromide) method as previously described<sup>16</sup>. All cell lines were maintained in RPMI1640 medium containing 10% FBS at 37°C in a 5% CO<sub>2</sub> humidified incubator. Cell proliferation assay was determined by the MTT method. Briefly, cells were passaged the day before dosing into a 96-well cell plate, allowed to grow for 12 h, and then treated with different concentrations of compound sample for 48 h. A 0.5% MTT solution was added to each well. After incubation for another 4 h, formazan

formed from MTT was extracted by adding 150  $\mu$ l of DMSO rocking for 15 min. Absorbance was then determined using an ELISA reader at 570 nm.

### 3. Results and Discussion

#### 3.1 Chemistry

Given the reports above, we decided to keep  $N^1$ -hydroxyterephthalamide with indole cap group as active structural fragments and designed compounds with different substituents, mainly including aliphatic amine and aromatic amine, to evaluate the impact of various functional groups on the inhibitory activities on HDACs. The synthesis of target compounds **8a-h** was described in **Scheme 1**. Briefly, the starting compound of *L*-tryptophan gave **2** by Boc-protection. Compound **2** was reacted with benzyl alcohol to give the ester intermediate **3**<sup>19</sup>. Deprotection followed by the coupling reaction with mono-methyl terephthalate in the presence of TBTU afforded **5**. Hydrogenation in the presence of Pd/C followed by ester amide exchange reaction produced target compound **8a**. On another route, coupling of **6** with various aliphatic amines followed by ester amide exchange reaction with acid yielded **8b-h** in good yield<sup>20</sup>. The synthesis of **12a-p** followed similar reactions to the synthetic method for compounds **8a-h**.

#### 3.2 HeLa cell extracts inhibition of the target compounds

As shown in the **Table 1**, within the aliphatic amide analogs, the chain length seemed to impact the potency dramatically with the shorter chain analog (**8b**) being more potent.

Compounds **8e-h** exhibited comparable potent on the inhibition of HDACs and this might suggest that steric or hydrophobic interactions were preferred at this specific position. The results of compounds **12b** and **12c** also supported this notion by showing sub-micromolar potency. Notably, aromatic amide analogs overall exhibited better inhibitory activities with the exception of compound **12p**. When the substitution pattern was compared within this

series, the para-substituted gave more potent analogs. Further evaluation revealed that halogenated analogs were preferred at this position and compound **12l** with para-iodine was the most potent one with nanomolar potency. This may suggest the substituent size is important at the para-position of the phenyl ring. To extend the confirmation of this notion, compounds **12m-p** were designed and evaluated. The results demonstrated that inhibitory potency of **12m** to HDACs was comparable to that of **12l** and compounds with more bulky substituents such as **12n-p** showed decreased potency. Collectively, this may suggest that the optimal size and at this position are needed to produce optimal interactions and consequently inhibitory activities.

### 3.3 Molecular docking of **12m** to HDAC2

In order to better understand the inhibition of **12m** to HDACs, docking studies were conducted employing structure of HDAC2. As shown in **Fig 3**, the linker of **12m** stretches to the bottom of the tunnel and the hydroxamic acid moiety orient can chelate properly with the zinc ion, which is consistent with the chelating type of **SAHA**. Compared to the sole hydrophobic interaction between the phenyl of **SAHA** and the amino acid residues around the external motif, the *p*-methylphenyl and the indole ring of **12m** can potentially double enhance the ligand–receptor bindings of the surface plot near the opening of the tunnel. In addition, the hydroxyl and carbonyl oxygens of **12m** have four H-bond interactions with His145, His146, Tyr308 and Asp104, while only two H-bond interactions of **SAHA** with His146 and Asp104 were displayed. Moreover, the benzene ring, as part linker of **12m**, has  $\pi$ - $\pi$  stacking interactions with the phenyl group of Phe155, which also improves its binding ability to the active site of HDAC2. All the information observed above could rationalize the better inhibitory activity of **12m** than **SAHA**.

### 3.4 HDAC isoform selectivity of **12m**

The studies employing the cellular extract demonstrated that compound **12m** was the most potent analog and slightly potent than **SAHA** under these experimental conditions. To further ascertain HDAC isoform-selectivity of **12m**, we conducted enzymatic inhibitory assays against HDAC1 (Class I), HDAC8 (Class I), HDAC6 (Class IIb), HDAC4 (Class IIa), and HDAC11 (Class IV). Compound **12m** exhibited almost no inhibition to HDAC4 at the concentration of 100  $\mu\text{M}$  and displayed  $\text{IC}_{50}$  values close to the magnitude of micromole or nanomole versus other HDAC isoforms, which demonstrated that **12m** showed similar overall selectivity profile with control **PXD101**.

### 3.5 *In vitro* antiproliferative assay

HDACs have been indicated significant roles in the proliferation and differentiation of cancer cells<sup>21,22</sup>. In the following research, we conducted *in vitro* antiproliferative evaluation of target compounds in cellular assays. Firstly, we tested the inhibition rate of all synthesized compounds at 5  $\mu\text{M}$  against two human leukemia cell lines (U937 and HEL)<sup>23</sup>. As the preliminary results showed in **Fig 4**, compounds **8d**, **12d**, **12j** and **12m** were selected as the representative ones for further antiproliferative evaluation *in vitro* against five frequently used cancer cell lines (**Table 3**) and exhibited comparable potency to **SAHA** in suppressing the growth of HL60 cells, but less inhibitory activities against other cell lines than **SAHA**. Interestingly, compound **8d** with less potent inhibition in cellular extracts assay, while overall displayed similar activities compared to **SAHA** *in vitro* antiproliferative assay. It was likely **8d** interacted with complicated binding sites in cancer cells of which main ingredients distinguished from the Hela cellular extracts.

## Conclusions

In this article, a series of  $N^1$ -hydroxyterephthalamide derivatives with indole cap analogs were designed, synthesized and biologically characterized as HDACIs. Compounds **12k**, **12l**, and **12m** displayed potent HDAC inhibitory activity compared with control drug **SAHA** *in vitro* HeLa cell extract inhibitory fluorescence assay. The most potent compound **12m** was also verified by molecular docking studies in the active site of HDAC2 and showed similar overall selectivity profile with control **PXD101** in HDAC isoform selectivity assay. Four selected compounds (**8d**, **12d**, **12j**, **12m**) demonstrated more potent or comparable antiproliferative activities to **SAHA** *in vitro* antiproliferative assay. We found antiproliferative activity of **12m** was less potent than **SAHA**, which was inferior to their enzyme inhibitory activity. One main reason could be that **12m** was limited by its poor transcellular permeability so that its specific binding with HDACs was weaker in cells. In addition, **12m** was likely to be disintegrated by other enzymes in cells before approaching active site of HDACs. To summarise, the results revealed that  $N^1$ -hydroxyterephthalamide with an indole cap could serve as novel chemical scaffold to develop more potent HDACIs.

## Acknowledgements

This work was supported by National Major Scientific and Technological Special Project for “Significant New Drugs Development” of China (Grant no. 2012ZX09103101-015).

## Conflict of interest

The authors declare no conflict of interest.

## References and notes

1. Sharma, S.; Kelly T. K.; Jones, P. A., Epigenetics in cancer. *Carcinogenesis* **2010**, *31*(1), 27-36.
2. Parbin, S., Kar, S., Shilpi, A., Sengupta, D., Deb, M., Rath, S. K., & Patra, S. K., Histone Deacetylases A Saga of Perturbed Acetylation Homeostasis in Cancer. *Journal of Histochemistry & Cytochemistry* **2014**, *62*(1), 11-33.
3. Dokmanovic, M.; Clarke, C.; Marks, P. A., Histone deacetylase inhibitors: overview and perspectives. *Molecular cancer research* **2007**, *5*(10), 981-989.
4. López, J. E.; Sullivan, E. D.; Fierke, C. A., Metal-dependent deacetylases: Cancer and epigenetic regulators. *ACS chemical biology* **2016**, *11*(3), 706-716.
5. Zhang L.; Han Y.; Jiang Q., et al. Trend of histone deacetylase inhibitors in cancer therapy: isoform selectivity or multitargeted strategy. *Medicinal research reviews* **2015**, *35*(1), 63-84.
6. Grant, S.; Easley, C.; Kirkpatrick, P., Vorinostat. *Nature reviews Drug discovery*, **2007**, *6*(1), 21-22.
7. McGraw, A. L., Romidepsin for the treatment of T-cell lymphomas. *American journal of health-system pharmacy : AJHP : official journal of the American Society of Health-System Pharmacists* **2013**, *70* (13), 1115-22.
8. Chan, D.; Zheng, Y.; Tyner, J. W.; Chng, W. J.; Chien, W. W.; Gery, S.; Leong, G.; Braunstein, G. D.; Koeffler, H. P., Belinostat and panobinostat (HDACI): in vitro and in vivo studies in thyroid cancer. *Journal of cancer research and clinical oncology* **2013**, *139* (9), 1507-14.
9. Gimsing, P., Belinostat: a new broad acting antineoplastic histone deacetylase inhibitor. *Expert opinion on investigational drugs* **2009**, *18* (4), 501-8.
10. Cheng, T.; Grasse, L.; Shah, J.; Chandra, J., Panobinostat, a pan-histone deacetylase inhibitor: rationale for and application to treatment of multiple myeloma. *Drugs of today* **2015**, *51* (8), 491-504.
11. Miller, T. A.; Witter, D. J.; Belvedere, S., Histone deacetylase inhibitors. *Journal of medicinal chemistry* **2003**, *46* (24), 5097-116.

12. Olson, D. E.; Wagner, F. F.; Kaya, T.; Gale, J. P.; Aidoud, N.; Davoine, E. L.; Lazzaro, F.; Weiwer, M.; Zhang, Y. L.; Holson, E. B., Discovery of the first histone deacetylase 6/8 dual inhibitors. *Journal of medicinal chemistry* **2013**, *56* (11), 4816-20.
13. DeSimone, R. W.; Currie, K. S.; Mitchell, S. A.; Darrow, J. W.; Pippin, D. A., Privileged structures: applications in drug discovery. *Combinatorial chemistry & high throughput screening* **2004**, *7* (5), 473-94.
14. Costantino, L.; Barlocco, D., Privileged structures as leads in medicinal chemistry. *Current medicinal chemistry* **2006**, *13* (1), 65-85.
15. Venugopal, B.; Baird, R.; Kristeleit, R. S.; Plummer, R.; Cowan, R.; Stewart, A.; Fourneau, N.; Hellemans, P.; Elsayed, Y.; McClue, S.; Smit, J. W.; Forslund, A.; Phelps, C.; Camm, J.; Evans, T. R.; de Bono, J. S.; Banerji, U., A phase I study of quisinostat (JNJ-26481585), an oral hydroxamate histone deacetylase inhibitor with evidence of target modulation and antitumor activity, in patients with advanced solid tumors. *Clinical cancer research : an official journal of the American Association for Cancer Research* **2013**, *19* (15), 4262-72.
16. Arts, J.; King, P.; Marien, A.; Floren, W.; Belien, A.; Janssen, L.; Pilatte, I.; Roux, B.; Decrane, L.; Gilissen, R.; Hickson, I.; Vreys, V.; Cox, E.; Bol, K.; Talloen, W.; Goris, I.; Andries, L.; Du Jardin, M.; Janicot, M.; Page, M.; van Emelen, K.; Angibaud, P., JNJ-26481585, a novel "second-generation" oral histone deacetylase inhibitor, shows broad-spectrum preclinical antitumoral activity. *Clinical cancer research : an official journal of the American Association for Cancer Research* **2009**, *15* (22), 6841-51.
17. Zhang, Y.; Yang, P.; Chou, C. J.; Liu, C.; Wang, X.; Xu, W., Development of -Hydroxycinnamamide-Based Histone Deacetylase Inhibitors with Indole-Containing Cap Group. *ACS medicinal chemistry letters* **2013**, *4* (2), 235-238.
18. Zhang Y.; Feng J.; Liu C.; Zhang L.; Jiao J.; Fang H.; Su L.; Zhang X.; Zhang J.; Li M.; Wang B.; Xu W., Design, synthesis and preliminary activity assay of 1, 2, 3, 4-tetrahydroisoquinoline-3- acid derivatives as novel Histone deacetylases (HDACs) inhibitors. *Bioorganic & medicinal chemistry* **2010**, *18*(5), 1761-1772.
19. Evans, M. J.; Morris, G. M.; Wu, J.; Olson, A. J.; Sorensen, E. J.; Cravatt, B. F., Mechanistic and structural requirements for active site labeling of phosphoglycerate mutase by spiroepoxides. *Molecular bioSystems* **2007**, *3* (7), 495-506.

20. Li, X.; Wu, J.; Li, X.; Mu, W.; Liu, X.; Jin, Y.; Xu, W.; Zhang, Y., Development of *N*-hydroxybenzamide derivatives with indole-containing cap group as histone deacetylases inhibitors. *Bioorganic & medicinal chemistry* **2015**, *23* (19), 6258-70.
21. Bolden, J. E.; Peart, M. J.; Johnstone, R. W., Anticancer activities of histone deacetylase inhibitors. *Nature reviews. Drug discovery* **2006**, *5* (9), 769-84.
22. Xu, W. S.; Parmigiani, R. B.; Marks, P. A., Histone deacetylase inhibitors: molecular mechanisms of action. *Oncogene* **2007**, *26* (37), 5541-52.
23. Li X.; Inks E. S.; Li X.; Hou J.; Chou C. J.; Zhang J.; Jiang Y.; Zhang Y.; Xu W., Discovery of the first *N*-hydroxycinnamamide-based histone deacetylase 1/3 dual inhibitors with potent oral antitumor activity. *Journal of medicinal chemistry* **2014**, *57*(8): 3324-3341.

## Supporting Information

Additional Supporting Information may be found in the online version of this article:

**Figure 1.** Pharmacophore model and HDACIs approved by FDA

**Figure 2.** Design of novel series of HDACIs

**Figure 3.** The docking modes of compounds **12m** (yellow molecular) and **SAHA** (green molecular) in the active site of HDAC2, derived by modification of PDB code 4LXZ with Tripos sybyl x 2.0 (Zinc ion is indicated green in the bottom of the tunnel)

**Figure 4.** Inhibition rate of synthesized compounds to U937 and HEL at 5  $\mu$ M

**Scheme 1.** The synthetic route for target compounds **8a-h** and **12a-p**.

**Table 1.** The chemical structures and HDACs inhibitory activities of *N*<sup>1</sup>-hydroxyterephthalamide Derivatives

**Table 2.** Inhibitory selectivity toward HDAC of compound **12m**.

**Table 3.** In vitro antiproliferative activity of **8d**, **12d**, **12j** and **12m**.

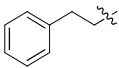
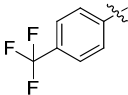
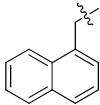
**Data S1.** Physical properties and spectrum data of target compounds.

This article is protected by copyright. All rights reserved.

## Tables

**Table 1.** The chemical structures and HDACs inhibitory activities of *N*<sup>1</sup>-hydroxyterephthalamide Derivatives

| Compd      | R | IC <sub>50</sub> <sup>a</sup> of Hela extract(μM) | Compd      | R | IC <sub>50</sub> <sup>a</sup> of Hela extract(μM) |
|------------|---|---|------------|---|---|
| <b>8a</b>  |   | 0.227   | <b>12f</b> |   | 0.360   |
| <b>8b</b>  |   | 1.654   | <b>12g</b> |   | 0.189   |
| <b>8c</b>  |   | 1.742   | <b>12h</b> |   | 0.435   |
| <b>8d</b>  |   | > 25  | <b>12i</b> |   | 0.202   |
| <b>8e</b>  |   | 0.527   | <b>12j</b> |   | 0.150   |
| <b>8f</b>  |   | 0.504   | <b>12k</b> |   | 0.096   |
| <b>8g</b>  |   | 0.683   | <b>12l</b> |   | 0.078   |
| <b>8h</b>  |   | 0.416   | <b>12m</b> |   | 0.074   |
| <b>12a</b> |   | 0.361   | <b>12n</b> |   | 0.413   |
| <b>12b</b> |   | 0.346   | <b>12o</b> |   | 0.335   |

|            |   |       |             |  |       |
|------------|---|-------|-------------|--|-------|
| <b>12c</b> |  | 0.301 | <b>12p</b>  |  | 1.287 |
| <b>12d</b> |  | 0.225 | <b>SAHA</b> |  | 0.131 |
| <b>12e</b> |  | 0.234 |             |  |       |

<sup>a</sup>Assays were performed in replicate ( $n \geq 2$ ); The SD values are  $< 20\%$  of the mean.

**Table 2.** Inhibitory selectivity toward HDAC of compound **12m**.

| compd          | IC <sub>50a</sub> ( $\mu$ M) |       |           |           |          |
|----------------|------------------------------|-------|-----------|-----------|----------|
|                | Class I                      |       | Class IIa | Class IIb | Class IV |
|                | HDAC1                        | HDAC8 | HDAC4     | HDAC6     | HDAC11   |
| <b>12m</b>     | 0.219                        | 5.50  | $>100$    | 0.168     | 3.50     |
| <b>PXD-101</b> | 0.034                        | 0.353 | 9.9       | 0.027     | 25       |

<sup>a</sup>Assays were performed in replicate ( $n \geq 2$ ); the SD values are  $< 20\%$  of the mean.

**Table 3.** In vitro antiproliferative activity of **8d**, **12d**, **12j** and **12m**.

| compd       | IC <sub>50</sub> <sup>a</sup> ( $\mu$ M) |                  |                  |                  |                  |
|-------------|--|------------------|------------------|------------------|------------------|
|             | K562                                     | U266             | KG-1             | HL60             | MCF-7            |
| <b>8d</b>   | 6.75 $\pm$ 0.96                          | 10.51 $\pm$ 0.96 | 2.63 $\pm$ 0.78  | 6.27 $\pm$ 0.46  | 3.25 $\pm$ 0.61  |
| <b>12d</b>  | 6.25 $\pm$ 0.07                          | 17.38 $\pm$ 1.57 | 10.23 $\pm$ 0.63 | 8.72 $\pm$ 0.06  | 12.59 $\pm$ 1.7  |
| <b>12j</b>  | 7.68 $\pm$ 0.53                          | 15.64 $\pm$ 0.64 | 8.05 $\pm$ 1.17  | 6.56 $\pm$ 0.13  | 7.07 $\pm$ 0.36  |
| <b>12m</b>  | 5.71 $\pm$ 0.20                          | 10.09 $\pm$ 0.41 | 9.09 $\pm$ 1.39  | 10.80 $\pm$ 0.33 | 13.33 $\pm$ 0.38 |
| <b>SAHA</b> | 1.76 $\pm$ 0.12                          | 1.98 $\pm$ 0.21  | 1.23 $\pm$ 0.14  | 9.37 $\pm$ 0.39  | 1.63 $\pm$ 0.29  |

<sup>a</sup>Assays were performed in replicate ( $n \geq 2$ ); the SD values are  $< 20\%$  of the mean.

